Journal of Quality Measurement and Analysis *JQMA* 22(1) 2026, 297-312
e-ISSN: 2600-8602 *http://www.ukm.my/jqma*
https://doi.org/10.17576/jqma.2201.2026.16

OPTIMIZATION OF TETRA HYBRID NANOFLUID FLOW OVER A CONVECTIVELY HEATED MOVING PLATE WITH HEAT GENERATION

(*Pengoptimuman Aliran Nanobendalir Tetra Hibrid Melewati Permukaan Bergerak yang Dipanaskan Secara Olakan dengan Penjanaan Haba)*

NAJIYAH SAFWA KHASHI'IE*, MOHD FARIDUDDIN MUKHTAR, MOHD FADZLI BIN ABDOLLAH, NORIHAN MD ARIFIN & IOAN POP

ABSTRACT

This study introduces a novel integrated computational and statistical approach for analyzing steady boundary layer flow and heat transfer in a tetra hybrid nanofluid containing alumina, copper, silica and titania nanoparticles dispersed in water past a convectively heated moving plate with internal heat generation. The governing nonlinear equations are reduced via similarity transformations and solved using Matlab's bvp4c solver to obtain highly accurate velocity, temperature, skin friction, and Nusselt number distributions. Response Surface Methodology (RSM) and sensitivity analysis are employed to quantify and rank the influence of heat generation, Biot number, and suction parameter. The numerical results reveal that increasing the Biot number may enhance the heat transfer rate by approximately 42.6 for opposing flow case and 53.6% for assisting flow case, whereas stronger wall suction improves heat transfer by about 0.5-6.2%. However, higher heat generation slightly weakens the heat transfer rate up to 3.6% and 0.2%, for opposing and assisting flow cases, respectively. The response surface methodology and sensitivity analysis also reveal that the Biot number exerts the dominant influence on heat transfer, followed by suction strength and heat generation rate. The principal novelty lies in the exclusive integration of numerical simulation with statistical optimization for a tetra hybrid nanofluid under convective heating, an area rarely addressed in the literature. The proposed framework not only identifies the most influential parameters but also determines optimal ranges for maximizing thermal performance. These findings establish a benchmark for designing advanced thermal management systems in high-temperature industrial and energy applications.

Keywords: convective boundary condition; heat generation; hybrid nanofluid; moving plate; response surface analysis; sensitivity analysis

ABSTRAK

Kajian ini memperkenalkan satu pendekatan bersepadu yang baharu melibatkan kaedah pengiraan berangka dan analisis statistik untuk meneliti aliran lapisan sempadan mantap serta ciri pemindahan haba dalam nanobendalir tetra hibrid yang terdiri daripada nanopartikel alumina (Al_2O_3), kuprum (Cu), silika (SiO_2) dan titania (TiO_2) yang terdispersi dalam air, mengalir melewati permukaan bergerak yang dipanaskan secara konvektif dengan kehadiran penjanaan haba dalaman. Persamaan tak linear yang mengawal selia fenomena ini diturunkan kepada bentuk persamaan transformasi keserupaan dan diselesaikan menggunakan penyelesai bvp4c dalam MATLAB bagi memperoleh taburan halaju, suhu, pekali geseran kulit dan nombor Nusselt dengan tahap ketepatan tinggi. Kaedah gerak balas permukaan (RSM) bersama analisis kepekaan digunakan untuk mengukur dan menyusun pengaruh parameter fizikal seperti penjanaan haba, nombor Biot dan parameter sedutan. Keputusan berangka menunjukkan bahawa peningkatan nombor Biot dapat meningkatkan kadar pemindahan haba secara ketara, iaitu sekitar 42.6% bagi kes aliran bertentangan dan 53.6% bagi kes aliran searah. Penguatan sedutan dinding pula memberikan peningkatan sederhana terhadap kadar pemindahan haba, iaitu antara 0.5% hingga 6.2%. Walau bagaimanapun, peningkatan parameter penjanaan haba didapati sedikit melemahkan kadar pemindahan haba masing-masing sebanyak 3.6% dan 0.2% bagi kes aliran bertentangan dan aliran searah. Dapatan ini mengesahkan bahawa nombor Biot memainkan peranan dominan dalam mempertingkatkan prestasi terma sistem, diikuti oleh parameter sedutan dan penjanaan haba yang memberi kesan sekunder terhadap profil suhu dan kadar penyejukan lapisan sempadan. Kaedah gerak balas permukaan bersama analisis kepekaan juga menunjukkan bahawa nombor Biot memberi kesan dominan terhadap pemindahan haba, diikuti oleh kekuatan sedutan dan kadar penjanaan haba. Keunikan utama kajian ini terletak pada pengintegrasian simulasi berangka dengan pengoptimuman statistik khusus untuk nanobendalir tetra hibrid di bawah pemanasan konvektif - suatu bidang yang masih jarang diterokai dalam literatur semasa. Rangka kerja yang dicadangkan bukan sahaja mengenal pasti parameter yang paling berpengaruh tetapi juga menentukan julat optimum untuk memaksimumkan prestasi terma. Penemuan ini menyediakan tanda aras penting bagi mereka bentuk sistem pengurusan haba canggih dalam aplikasi industri dan tenaga bersuhu tinggi.

Kata kunci: syarat sempadan konvektif; penjanaan haba; nanobendalir hibrid; permukaan bergerak; analisis gerak balas permukaan; analisis kepekaan

1. Introduction

Efficient heat transfer plays an important role in maintaining the thermal stability of engineering systems particularly in applications where precise cooling or heating is essential to ensure safe operational limits. In various industrial processes, the effective management of excess heat is crucial for sustaining optimal performance and preventing thermally induced failures. Conventional liquid coolants have long been utilized for this purpose (Zhang *et al.* 2021). However, their relatively low thermal conductivity significantly limits their capacity to dissipate heat efficiently. To overcome this limitation, nanofluids have been proposed as advanced heat transfer media. These fluids are engineered colloidal suspensions in which nanoparticles comprising metals, non-metals or metal oxides are uniformly dispersed within a base fluid (Choi & Eastman 1995). The inclusion of thermally conductive nanoparticles such as copper, in the base fluid can substantially enhance thermal conductivity and overall heat transfer characteristics, thereby improving the coolant's performance in advanced thermal management applications. The thermal behaviour of such nanofluids is strongly influenced by both the particle size and volume fraction of the dispersed nanoparticles (Maruda *et al.* 2023). While the addition of nanoparticles generally enhances heat transfer capability, careful optimization of their concentration is essential as excessive loading can result in particle agglomeration and sedimentation which leading to instability and reduced thermal performance. Nanofluids can be broadly classified into two main categories; single nanofluids in which a single type of nanoparticle is dispersed in the base fluid, and hybrid nanofluids which incorporate two or more distinct nanoparticles within the same fluid medium, offering the potential for synergistic enhancement of thermophysical properties as discussed by Modi *et al*. (2023). Numerous investigations have demonstrated the effectiveness of nanofluids in improving convective heat transfer performance particularly in boundary layer flow configurations (Sahoo & Kumar 2020; Reddy & Reddy 2015; Maskeen *et al.* 2019; Yan *et al.* 2020; Zainal *et al.* 2021; Khashi'ie *et al.* 2022).

Tetra hybrid nanofluids which are composed of four distinct types of nanoparticles may offer a promising extension to conventional and binary (dual/ternary) hybrid nanofluids by enabling more precise manipulation of thermophysical properties such as thermal conductivity, dynamic viscosity, and overall dispersion stability. Elsherbiny *et al.* (2025)

experimentally studied the performance of Al_2O_3-CuO-ZnO-Ag/distilled water nanofluid in a microprocessor cooling system. The highest heat flux and flow velocity was recorded by Al_2O_3-ZnO-Ag ternary nanofluid, however, maximum enhancement values of Nusselt number are not an exclusive thing for higher levels of hybrid nanofluids as Al_2O_3 mono nanofluid recorded the highest enhancement value over all tested nanofluids. Further complementary numerical contributions on tetra hybrid nanofluid behaviours under diverse configurations are available in the studies conducted by Khan *et al.* (2024), Mahariq *et al.* (2024) and Oladapo *et al.* (2024).

Many researchers have opted numerical techniques and very recent, statistical data analysis and optimization in examining the boundary layer flow including the changes in input parameters which affect the flow behaviour and solution. Numerical analysis involves developing and applying computational methods to solve the governing boundary layer model, while the statistical data analysis like sensitivity analysis identifies which factors most strongly influence the boundary layer characteristics. Shutaywi *et al.* (2024) used Fuzzy TOPSIS method to optimize heat transfer of tetra hybrid nanofluid within a channel. Meanwhile, Venkatadri *et al.* (2024) analyzed the non-Darcy flow in TiO2/Cu–water hybrid nanofluid subjected to a differentially heated square enclosure using both numerical analysis (Lattice Boltzmann Method) and RSM with sensitivity analysis. Further, both RSM and sensitive analysis were also used by Panda *et al.* (2023) in the optimization of the heat transfer rate on the problem related to the MHD hybrid nanofluid flow subjected to a convectively heated expanding/contracting surface saturated in a porous medium. Other papers which reported and utilized statistical data analysis as well as the optimization and sensitivity analysis can be found in these references (Mehmood *et al.* 2021; Mahanthesh & Thriveni 2021; Vahedi *et al.* 2018; Abdelmalek *et al.* 2020; Wahid *et al.* 2024, 2025a, 2025b; Yahaya *et al.* 2024, 2025; Alsemiry *et al.* 2025; Khashi'ie *et al.* 2023, 2025).

In this study, we address these gaps by integrating the bvp4c numerical solver with RSM-based sensitivity analysis. This combination allows us not only to solve the PDEs governing nanofluid flow but also to determine the most influential physical factors affecting heat transfer such as the heat generation parameter, suction effect and Biot number (represent the convective heating). This dual approach provides a deeper understanding of the parameter sensitivity, thus offering a more comprehensive solution to optimizing nanofluid flow systems. Previous studies, while successful in solving the governing equations of nanofluid flow, often lacked a comprehensive statistical approach that could highlight the sensitivity of various physical parameters to the system's heat transfer performance. For instance, while numerical solutions can predict how different physical factors influence heat transfer, they do not provide insights into which parameters have the most significant impact. Additionally, most previous works did not integrate numerical solutions with response surface methodology (RSM) or sensitivity analysis, limiting their ability to identify optimal conditions for enhanced thermal performance.

To address these research gaps, the present work conducts a numerical investigation of tetra hybrid nanofluid consisting of alumina, copper, silica and titania nanoparticles dispersed in water over a convectively heated moving plate with the presence of heat generation. The governing equations, derived via similarity transformations, are solved using the MATLAB bvp4c solver which provides accurate and efficient solutions for the coupled nonlinear differential equations. The novelty of this study lies in its focused numerical and statistical examination of the thermophysical behaviour of a tetra hybrid nanofluid under convective heating, an area that has received limited attention in existing literature. In this work, we used the above stated nanoparticles because of each nanoparticles' strength. Al_2O_3 provides excellent thermal stability and cost effectiveness which ensuring long-term stability of the suspension. Cu exhibits high thermal conductivity which improving heat transfer capacity, though its tendency to agglomerate requires balancing with stabilizing oxides. SiO_2 enhances dispersion stability, reduces sedimentation and contributes to improved rheological properties of the suspension due to its low density. TiO_2 contributes chemical resistance and radiative responsiveness, making it suitable for high-temperature and radiation environments. The combination of these four nanoparticles creates a synergistic formulation in which the high thermal conductivity of Cu is complemented by the stabilizing effect of SiO_2 and Al_2O_3, while TiO_2 enhances thermal performance under radiative conditions. This balance ensures simultaneous improvements in heat transfer efficiency, suspension stability and resistance to agglomeration. The findings offer valuable insight into the influence of the physical parameters on flow dynamics and thermal performance, establishing a computational benchmark for future research in advanced heat transfer enhancement with potential applications.

2. Mathematical Model

This study investigates the heat transfer and flow characteristics of alumina-copper-silica-titania/water tetra hybrid nanofluid past a moving plate with heat generation. The coordinate system follows a Cartesian configuration (refer to Figure 1), where the x-axis extends along the heated surface and the y-axis acts normal to it, penetrating into the fluid layer. The tetra hybrid nanofluid is assumed to flow with a uniform free-stream velocity U, while the plate velocity is defined by λU. Here, $\lambda > 0$ signifies motion in the direction of the main stream, and $\lambda > 0$ denotes counter-motion relative to the flow. In addition, the surface temperature of the moving plate, T_f is maintained through convective heating by an external fluid characterized by a constant heat transfer coefficient $h_{f1}(x) = h_f / \sqrt{x}$ where h_f is a constant. The ambient temperature, T_∞ is taken as spatially uniform, following the formulations of Yaseen *et al.* (2021) and Wahid *et al.* (2025c). The proposed configuration facilitates heat transfer enhancement analysis and enables quantitative sensitivity assessment of key governing parameters by employing the Response Surface Methodology (RSM) framework.

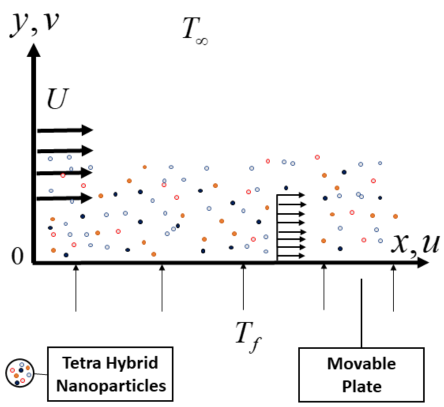

Figure 1: Illustration of the model

Within the adopted simplifications, the governing set (Eqs. (1)-(4)) originates from conservation of momentum and energy are derived. The standard boundary-layer equations have been extended to include the effects of heat generation, convective thermal boundary conditions and wall suction appropriate for the tetra-hybrid nanofluid configuration. The methodology is grounded in the developments of Khashi'ie *et al.* (2022) and Weidman *et al.* (2006), thereby ensuring that the model remains consistent with boundary-layer assumptions as well as enhanced thermal-transport modelling in nanoscale fluids.

$$\frac{\partial u}{\partial x}+\frac{\partial v}{\partial y}=0, \tag{1}$$

$$u\frac{\partial u}{\partial x}+v\frac{\partial u}{\partial y}=\frac{\mu_{ttnf}}{\rho_{ttnf}}\frac{\partial^2 u}{\partial y^2}, \tag{2}$$

$$u\frac{\partial T}{\partial x}+v\frac{\partial T}{\partial y}=\frac{k_{ttnf}}{(\rho C_p)_{ttnf}}\frac{\partial^2 T}{\partial y^2}+\frac{Q_1}{(\rho C_p)_{ttnf}}\left(T-T_\infty\right), \tag{3}$$

$$\begin{gathered} u=\lambda U,\quad v=v_w,\quad -k_{ttnf}\frac{\partial T}{\partial y}=h_f\left(T_f-T\right)\quad \text{at}\quad y=0 \\ u\to U,\quad T\to T_\infty \quad \text{as}\quad y\to\infty \end{gathered} \tag{4}$$

The fluid velocities are u ($x-$axis) and v ($y-$axis), respectively, $Q_1=Q_0x^{-1}$ is the heat generation function where Q_0 is a constant (Yaseen *et al.* 2021; Wahid *et al.* 2025c) and T is the tetra hybrid nanofluid's temperature. In addition, the boundary conditions in Eq. (4) specify the behavior of the flow at the moving wall $(y=0)$ and in the free stream $(y\to\infty)$. The surface mass flow is $v_w=-\sqrt{\frac{Uv_f}{2x}}S,$ where the suction parameter S is incorporated into the formulation to aid in stabilizing the boundary-layer flow, especially when reverse flow or flow separation tendencies occur. In this configuration, the convective heating mechanism couples the thermal flux at the wall with the temperature disparity between the surface and the external fluid medium, governed by the heat transfer coefficient $h_{f1}(x)$. Table 1 shows the thermophysical properties of the Al_2O_3 (ϕ_1), Cu (ϕ_2), SiO_2 (ϕ_3), TiO_2 (ϕ_4) and water, respectively while Table 2 presents the correlations for the tetra hybrid nanofluid, adopted from Khan *et al.* (2024) and Mahariq *et al.* (2024).

Table 1: Thermophysical properties

Physical properties	Water	TiO_2	SiO_2	Cu	Al_2O_3
k(W/mK)	0.6130	8.9538	1.4013	400	40
ρ(kg/m^3)	997.1	4250	2200	8933	3970
C_p(J/kgK)	4179	686.2	754	385	765

Table 2: Correlations of tetra hybrid nanofluids

Properties	Correlations
Density	$\rho_{ttnf} = (1-\phi_4)\left\{(1-\phi_3)\left[(1-\phi_2)\left((1-\phi_1)\rho_f + \phi_1\rho_{s1}\right) + \phi_2\rho_{s2}\right] + \phi_3\rho_{s3}\right\} + \phi_4\rho_{s4}$
Thermal Conductivity	$k_{ttnf} = k_{thnf}\left[\dfrac{k_{s4} + 2k_{thnf} - 2\phi_4\left(k_{thnf} - k_{s4}\right)}{k_{s4} + 2k_{thnf} + \phi_4\left(k_{thnf} - k_{s4}\right)}\right]$ where $k_{thnf} = k_{hnf}\left[\dfrac{k_{s3} + 2k_{hnf} - 2\phi_3\left(k_{hnf} - k_{s3}\right)}{k_{s3} + 2k_{hnf} + \phi_3\left(k_{hnf} - k_{s3}\right)}\right]$, $k_{hnf} = k_{nf}\left[\dfrac{k_{s2} + 2k_{nf} - 2\phi_2\left(k_{nf} - k_{s2}\right)}{k_{s2} + 2k_{nf} + \phi_2\left(k_{nf} - k_{s2}\right)}\right]$, $k_{nf} = k_f\left[\dfrac{k_{s1} + 2k_f - 2\phi_1\left(k_f - k_{s1}\right)}{k_{s1} + 2k_f + \phi_1\left(k_f - k_{s1}\right)}\right]$.
Dynamic Viscosity	$\mu_{ttnf} = \dfrac{\mu_f}{\left\{(1-\phi_1)(1-\phi_2)(1-\phi_3)(1-\phi_4)\right\}^{2.5}}$
Heat Capacity	$\left(\rho C_p\right)_{ttnf} = (1-\phi_4)\left\{\begin{matrix}(1-\phi_3)\left[(1-\phi_2)\begin{pmatrix}(1-\phi_1)\left(\rho C_p\right)_f \\ +\phi_1\left(\rho C_p\right)_{s1}\end{pmatrix} + \phi_2\left(\rho C_p\right)_{s2}\right] \\ +\phi_3\left(\rho C_p\right)_{s3}\end{matrix}\right\} + \phi_4\left(\rho C_p\right)_{s4}$

Following Yaseen *et al.* (2021) and Wahid *et al.* (2025c), the similarity transformations is

$$\left.u = Uf'(\eta),\quad v = \sqrt{\frac{U\nu_f}{2x}}\left(\eta f' - f\right),\quad \eta = \sqrt{\frac{U}{2x\nu_f}}\,y,\quad \psi = \sqrt{2\nu_f xU}\,f(\eta),\quad \theta(\eta) = \frac{T - T_\infty}{T_w - T_\infty}\right\} \tag{5}$$

By applying the similarity transformations defined in Eq. (5) to Eqs. (2)-(4), and ensuring compliance with the continuity constraint expressed in Eq. (1), the governing equations are reduced to the following system

$$\left(\frac{\mu_{ttnf}/\mu_f}{\rho_{ttnf}/\rho_f}\right) f''' + ff'' = 0, \tag{6}$$

$$\frac{1}{\Pr}\frac{k_{ttnf}/k_f}{\left(\rho C_p\right)_{ttnf}/\left(\rho C_p\right)_f}\theta'' + f\theta' + \frac{2Q\theta}{\left(\rho C_p\right)_{ttnf}/\left(\rho C_p\right)_f} = 0, \tag{7}$$

$$\begin{gathered} f'(0) = \lambda,\quad f(0) = S,\quad \frac{-k_{ttnf}}{k_f}\theta'(0) = Bi\left[1 - \theta(0)\right], \\ f'(\infty) = 1,\quad \theta(\infty) = 0. \end{gathered} \tag{8}$$

The dimensionless parameters are:
(i) Q denotes the heat generation parameter,
(ii) $\Pr$ represents the Prandtl number, and
(iii) Bi corresponds to the Biot number.

These parameters are mathematically defined as:

$$Q = \frac{Q_0}{U\left(\rho C_p\right)_f}, \quad \Pr = \frac{\left(\mu C_p\right)_f}{k_f}, \quad Bi = \sqrt{\frac{2\nu_f}{U}}\frac{h_f}{k_f}. \tag{9}$$

The skin friction coefficient and the local Nusselt number are

$$C_f = \frac{\mu_{ttnf}}{\rho_f U^2}\left(\frac{\partial u}{\partial y}\right)_{y=0}, \quad Nu_x = -\frac{x k_{ttnf}}{k_f\left(T_f - T_\infty\right)}\left(\frac{\partial T}{\partial y}\right)_{y=0}. \tag{10}$$

The application of the similarity variables in Eq. (5) into Eq. (10) yields the reduced formulations for both the skin friction coefficient and the local Nusselt number (see Yaseen *et al.* 2021; Wahid *et al.* 2025c)

$$\sqrt{2}\,\mathrm{Re}_x^{1/2} C_f = \frac{\mu_{ttnf}}{\mu_f} f''(0), \quad \sqrt{2}\,\mathrm{Re}_x^{-1/2} Nu_x = -\frac{k_{ttnf}}{k_f}\theta'(0), \quad \mathrm{Re}_x = xU/\nu_f. \tag{11}$$

3. Numerical Solutions

Equations (6)-(8) was solved to evaluate the effects of the governing parameters on the skin friction coefficient and the local Nusselt number, which represent the shear stress at the wall and the rate of heat transfer, respectively. The Matlab bvp4c solver is applicable to obtain the solutions due to its robustness in handling nonlinear boundary value problems, particularly those involving mixed-type boundary conditions and multiple solution branches. The bvp4c solver incorporates an adaptive mesh refinement strategy that automatically adjusts the discretization points in regions of steep gradients, thereby improving accuracy and computational efficiency. The numerical process begins by reformulating Eqs. (6)-(8) into a system of first order ODEs, as shown in Eqs. (12)-(14), and implementing them in a dedicated Matlab function file. Appropriate modifications such that $f = y(1), f' = y(2), f'' = y(3),\ \theta = y(4),\ \theta' = y(5)$ ensures the numerical stability. The solver iteratively refined the mesh until the residuals satisfied the predefined convergence tolerance which offering reliable and accurate solutions for both the velocity and temperature profiles.

$$f''' = \frac{\rho_{ttnf}/\rho_f}{\mu_{ttnf}/\mu_f}\left(-y(1)y(3)\right), \tag{12}$$

$$\theta'' = \Pr\frac{\left(\rho C_p\right)_{ttnf}/\left(\rho C_p\right)_f}{\left(k_{ttnf}/k_f\right)}\left(-y(1)y(5) - \frac{2Qy(4)}{\left(\rho C_p\right)_{ttnf}/\left(\rho C_p\right)_f}\right), \tag{13}$$

$$ya(2)-\lambda,\ \ ya(1)-S,\ \ \frac{-k_{ttnf}}{k_f}ya(5)=Bi\left[1-ya(4)\right], \\ yb(2),\ \ yb(4). \tag{14}$$

To validate the accuracy and reliability of the present numerical results, the current model is reduced to a special case for which data are available in the literature. The computed values of the $f''(0)$ were compared with the numerical results reported by Wahid et al. (2025c) and Zainal *et al*. (2021), and an excellent agreement was observed as presented in Table 3. This close correlation confirms the correctness of the present numerical scheme and the appropriateness of the bvp4c solver for solving the governing boundary value problem.

Table 3: Validation of numerical values $f''(0)$ when $\phi_2 = 0.1$ (copper), $S=\phi_1=\phi_3=0$ and $Bi\to\infty$

	Present		Wahid *et al*. (2025c)		Zainal *et al*. (2021)	
λ	First	Second	First	Second	First	Second
-0.20	0.505318	0.026061	0.505317779	0.026061434	0.505318	0.026061
-0.25	0.471688	0.053322	0.471688345	0.026061434	0.471688	0.053322
-0.30	0.418959	0.099702	0.418959116	0.026061434	0.418959	0.099702
-0.35	0.302592	0.209761	0.302592535	0.026061434	0.302592	0.209761

4. Response Surface Methodology and Sensitivity Analysis

Equations (6)-(8) was solved to evaluate the effects of the governing parameters on the skin friction coefficient and the local Nusselt number, which represent the shear stress at the wall and the rate of heat transfer, respectively. The Matlab bvp4c solver is applicable to obtain the solutions due to its robustness in handling nonlinear boundary value problems, particularly those involving The present section discusses the application of the Response Surface Methodology (RSM) to the numerical results obtained in the preceding analysis. The objective is to elucidate the individual and combined effects of the suction strength, Biot number and heat generation parameter on the performance of the tetra hybrid nanofluid boundary layer. As a Design of Experiment (DOE) technique, RSM enables a structured and quantitative assessment of these parameters, thereby identifying their relative contributions to the heat-transfer rate and flow stability. To implement the analysis, a Central Composite Design (CCD) comprising 20 simulation runs and three control factors: heat generation, Biot number, and suction is employed (see Table 4). The CCD layout ensures both statistical robustness and computational efficiency in exploring the multi-dimensional design space. In Table 4, the real values are the actual parameter values that are substituted into the governing equations and solved using the bvp4c solver in the Matlab software. Meanwhile, the coded values correspond to their normalized, dimensionless equivalents adopted in the Response Surface Methodology (RSM) to facilitate statistical analysis and regression modeling. This statistical framework enables a more comprehensive interpretation of the governing thermo-hydrodynamic mechanisms in the tetra hybrid nanofluid facilitating the enhancement and optimization of overall thermal efficiency.

From Table 4, the increasing value of Biot number may enhance the heat transfer rate by approximately 42.6 for opposing flow case $(\lambda_1=-0.7)$ and 53.6% for assisting flow case $(\lambda_2=0.7)$, whereas stronger wall suction improves heat transfer by about 6.2% $(\lambda_1=-0.7)$

and 0.5% $(\lambda_2 = 0.7)$. Conversely, higher heat generation slightly weakens the heat transfer rate up to 3.6% $(\lambda_1 = -0.7)$ and 0.2% $(\lambda_2 = 0.7)$. The two Pareto charts in Figure 2 compare the standardized effects of factors A, B, and C on the heat transfer for both cases $\lambda_1 = -0.7$ and $\lambda_2 = 0.7$. For case λ_1 as in Figure 2a, Factor B has the strongest effect, followed by Factor C. The quadratic term BB and Factor A also contribute moderately, while interaction terms (BC, AC) and other quadratic effects (CC, AA) are negligible. Only B, C, BB, and A appear statistically significant, likely exceeding the redline threshold. In the heat transfer chart for case λ_2 as in Figure 2b, Factor B dominates with an extremely high standardized effect, far surpassing all other terms. BB and Factor C also show notable influence, while Factor A and interaction effects are minor. Again, higher-order terms (CC, AA) have little impact, with only B, BB, and C likely crossing the significance threshold.

Table 4: Experimental design for the heat transfer rate (first stable solution)

Run	Real			Coded				
	Q	Bi	S	A	B	C	$\lambda_1 = -0.7$	$\lambda_2 = 0.7$
1	0.03	1	0.52	1	-1	1	0.640104860	0.804866413
2	0.02	2	0.51	0	0	0	0.935071091	1.343881557
3	0.01	1	0.52	-1	-1	1	0.663504079	0.806639926
4	0.01	2	0.51	-1	0	0	0.962893193	1.346410626
5	0.02	2	0.52	0	0	1	0.968697112	1.349411081
6	0.03	2	0.51	1	0	0	0.903265667	1.341315317
7	0.02	3	0.51	0	1	0	1.107700941	1.731762076
8	0.01	3	0.5	-1	1	-1	1.098075371	1.726754600
9	0.02	2	0.51	0	0	0	0.935071091	1.343881557
10	0.02	1	0.51	0	-1	0	0.637171003	0.803785381
11	0.02	2	0.51	0	0	0	0.935071091	1.343881557
12	0.02	2	0.5	0	0	-1	0.895566947	1.338273321
13	0.03	3	0.5	1	1	-1	1.000621821	1.718107184
14	0.01	1	0.5	-1	-1	-1	0.633974322	0.802704952
15	0.02	2	0.51	0	0	0	0.935071091	1.343881557
16	0.01	3	0.52	-1	1	1	1.189791942	1.745067155
17	0.03	1	0.5	1	-1	-1	0.600223804	0.800831242
18	0.02	2	0.51	0	0	0	0.935071091	1.343881557
19	0.03	3	0.52	1	1	1	1.116598098	1.736787928
20	0.02	2	0.51	0	0	0	0.935071091	1.343881557

The regression equations for the heat transfer of both cases are as follows:

$$\begin{aligned}\lambda_1 = {} & 0.93502 - 0.02874A + 0.23378B + 0.03502C - 0.00186A^2 \\ & - 0.06251B^2 - 0.00281C^2 + 0.00433AC + 0.01729BC\end{aligned} \tag{15}$$

$$\begin{aligned}\lambda_2 = {} & 1.34388 - 0.002567A + 0.463965B + 0.005610C - 0.000017A^2 \\ & - 0.076106B^2 - 0.000038C^2 + 0.000059AC + 0.003628BC\end{aligned} \tag{16}$$

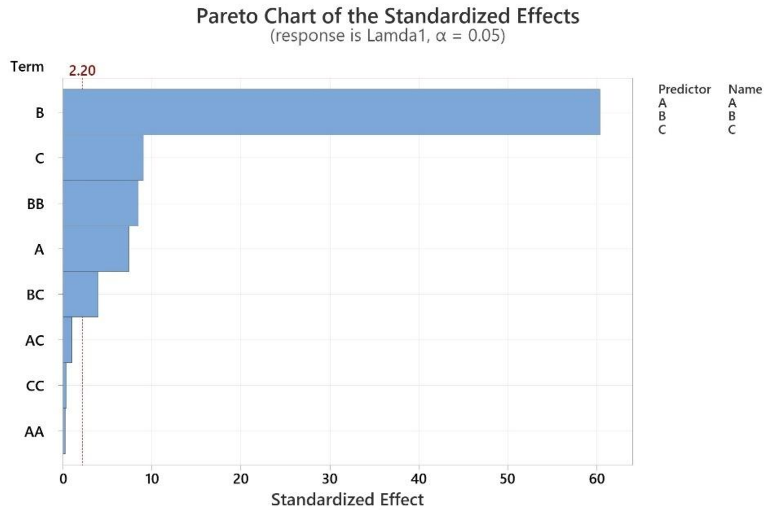

(a)

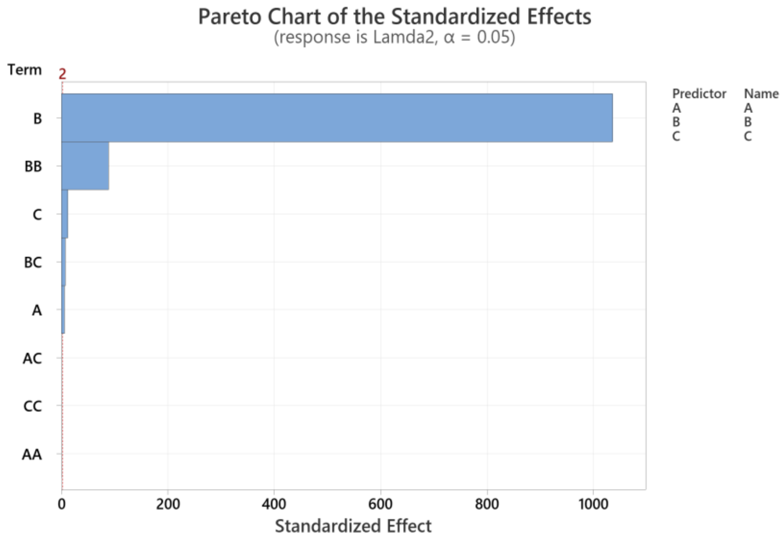

(b)

Figure 2: Influence of the parameters on heat transfer based on the statistical data analysis when (a) $\lambda_1 = -0.7$ and (b) $\lambda_2 = 0.7$

The sensitivity equations are based on Eqs. (15) and (16) such that

$$\begin{aligned} \frac{\partial(\lambda_1)}{\partial \mathrm{A}} &= -0.02874 - 2(0.00186)A + 0.00433C, \\ \frac{\partial(\lambda_1)}{\partial \mathrm{B}} &= 0.23378 - 2(0.06251)B + 0.01729C, \\ \frac{\partial(\lambda_1)}{\partial \mathrm{C}} &= 0.03502 - 2(0.00281)C + 0.00433A + 0.01729B. \end{aligned} \tag{17}$$

$$\frac{\partial(\lambda_2)}{\partial \mathrm{A}} = -0.002567 - 2(0.000017)A + 0.000059C,$$
$$\frac{\partial(\lambda_2)}{\partial \mathrm{B}} = 0.463965 - 2(0.076106)B + 0.003628C, \tag{18}$$
$$\frac{\partial(\lambda_2)}{\partial \mathrm{C}} = 0.005610 - 2(0.000038)C + 0.000059A + 0.003628B.$$

Table 5 reports the ANOVA findings for the heat transfer for case λ_1, providing a comparative assessment of the importance of individual factors and their interactions. The results indicate that Factor B exerts the most pronounced effect, reflected by an exceptionally high F-value of 3646.29 and a corresponding p-value of 0.000, signifying a statistically significant contribution to the response. Factor C also shows statistical significance (F = 81.84, P = 0.000), whereas Factor A contributes moderately (F = 55.12, P = 0.000). Among the squared terms, B^2 is the only one with a significant effect (F = 71.68, P = 0.000), suggesting a nonlinear impact of B on the response. All other quadratic and interaction terms including A^2, C^2, and AC are insignificant, with P-values above 0.3, indicating negligible contributions. However, the interaction term BC is statistically significant (F = 15.95, P = 0.002), implying that the joint effect of B and C should not be overlooked. The regression model as a whole is highly significant (F = 492.85, P = 0.000), and the low residual error (Adj SS = 0.001649) demonstrates a strong model fit.

Table 5: ANOVA for λ_1

Source	DF	Adj SS	Adj MS	F-Value	P-Value
Regression	8	0.590978	0.073872	492.85	0.000
A	1	0.008261	0.008261	55.12	0.000
B	1	0.546536	0.546536	3646.29	0.000
C	1	0.012266	0.012266	81.84	0.000
A*A	1	0.000010	0.000010	0.06	0.806
B*B	1	0.010744	0.010744	71.68	0.000
C*C	1	0.000022	0.000022	0.14	0.711
A*C	1	0.000150	0.000150	1.00	0.339
B*C	1	0.002390	0.002390	15.95	0.002
Error	11	0.001649	0.000150		
Lack-of-Fit	6	0.001649	0.000275	*	*
Pure Error	5	0.000000	0.000000		
Total	19	0.592627			

Figure 3 provides a visual representation of the individual value plots for the heat transfer for case λ_1 in relation to factors B and C. The top left panel shows the overall influence of C, which appears to be minimal, as the mean values remain relatively constant across the three levels. This aligns with the statistical result that C, while significant, has a smaller effect compared to B. The breakdown by B (top right panels) shows a clear increase in case of λ_1 as B increases, especially when B = 1, reinforcing its dominant role. Meanwhile, changes across C levels are less pronounced, indicating a relatively weaker impact. The bottom left plot reveals a clear upward trend in the score by B, confirming the strong linear relationship between B and the response. The breakdown by C (bottom right panels) maintains this trend across all C levels, with higher B values consistently yielding higher heat transfer values for λ_1, suggesting the effect of B is robust across varying C levels. This also visually supports the significance of the BC interaction, as the slope slightly changes between C levels. Error bars across plots indicate some variability but are not wide enough to challenge the significance of B's effect. In summary, both the ANOVA results and the individual value plots corroborate that Factor B is the most influential on case of λ_1, followed by Factor C and Factor A, while BC is the only interaction that has a meaningful effect. The visual and statistical analyses jointly support the conclusion that B has a strong, consistent, and slightly nonlinear impact on the heat transfer of case λ_1, with minimal interference from other factors.

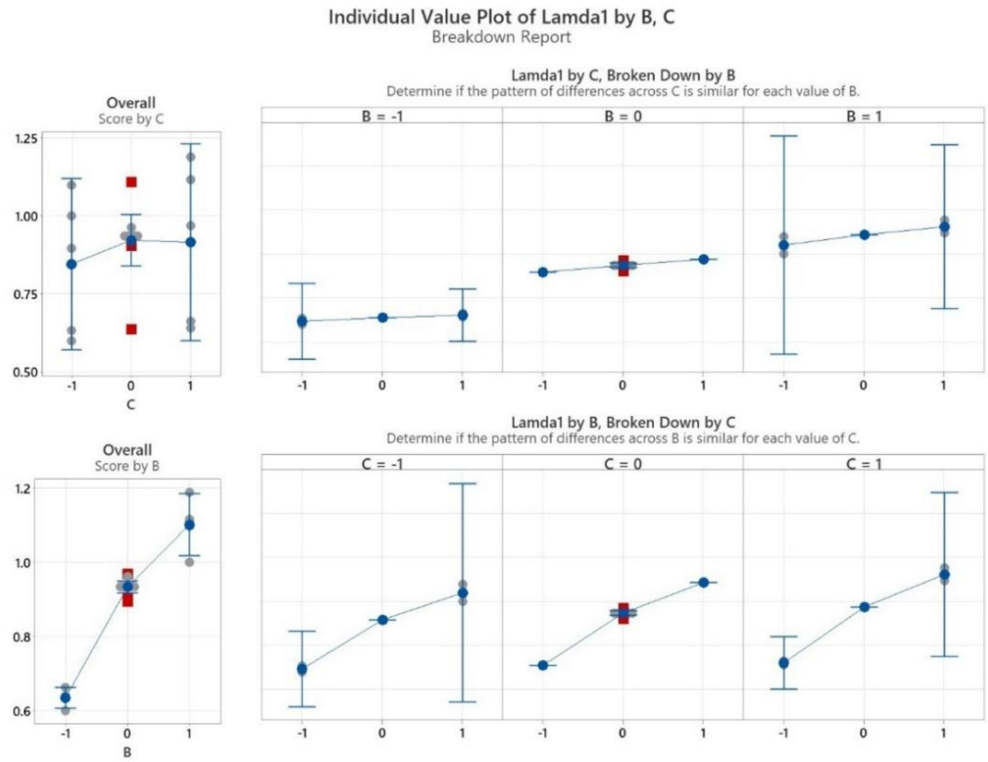

Figure 3: Sensitivity Analysis for case $\lambda_1 = -0.7$

Table 6 presents the results of the ANOVA for the regression model, which evaluates the effects of factors A, B, and C including their interactions and quadratic terms on the heat transfer for case λ_2. The overall model is highly significant (F = 136020.74, p < 0.001), indicating a strong fit. Among all predictors, factor B emerges as the most influential variable with a remarkably high F-value of 1,073,469.01 (p < 0.001), followed by its quadratic term BB (F = 7943.16, p < 0.001), signifying both linear and nonlinear effects. Factor C also contributes significantly to the model (F = 156.95, p < 0.001), as does the interaction term BC (F = 52.51, p < 0.001), albeit with smaller effect sizes. In contrast, factor A, its square term AA, and the interaction term AC show no statistically significant influence (p > 0.05), indicating that A has a negligible effect on λ_2 within the studied range.

These statistical findings are visually supported by the individual value plots of λ_1 and λ_2. For λ_1, the plot of Score by B reveals a clear increasing trend, affirming the strong main effect of B observed in the ANOVA. The plot of Score by C shows a modest curvature, aligning with the significant but less dominant effect of C. Breakdown plots demonstrate that the influence of B remains consistent across different levels of C, while the interaction between B and C introduces slight shifts in slope, visually reflecting the statistically significant BC term. Similarly, the plots for λ_2 further reinforce the dominant effect of B. Across all levels of C, λ_2 increases consistently with B, supporting the high F-values for both B and BB. The Score by C plot continues to show moderate variation, while the interaction plots indicate a subtle but consistent BC interaction. Factor A exhibits minimal variation across levels in both λ_1 and λ_2 plots, visually confirming its lack of statistical significance.

Table 6: ANOVA of λ_2

Source	DF	Adj SS	Adj MS	F-Value	P-Value
Regression	8	2.18211	0.27276	136020.74	0.000
A	1	0.00007	0.00007	32.86	0.000
B	1	2.15264	2.15264	1073469.01	0.000
C	1	0.00031	0.00031	156.95	0.000
A*A	1	0.00000	0.00000	0.00	0.984
B*B	1	0.01593	0.01593	7943.16	0.000
C*C	1	0.00000	0.00000	0.00	0.965
A*C	1	0.00000	0.00000	0.01	0.909
B*C	1	0.00011	0.00011	52.51	0.000
Error	11	0.00002	0.00000		
Lack-of-Fit	6	0.00002	0.00000	*	*
Pure Error	5	0.00000	0.00000		
Total	19	2.18213			

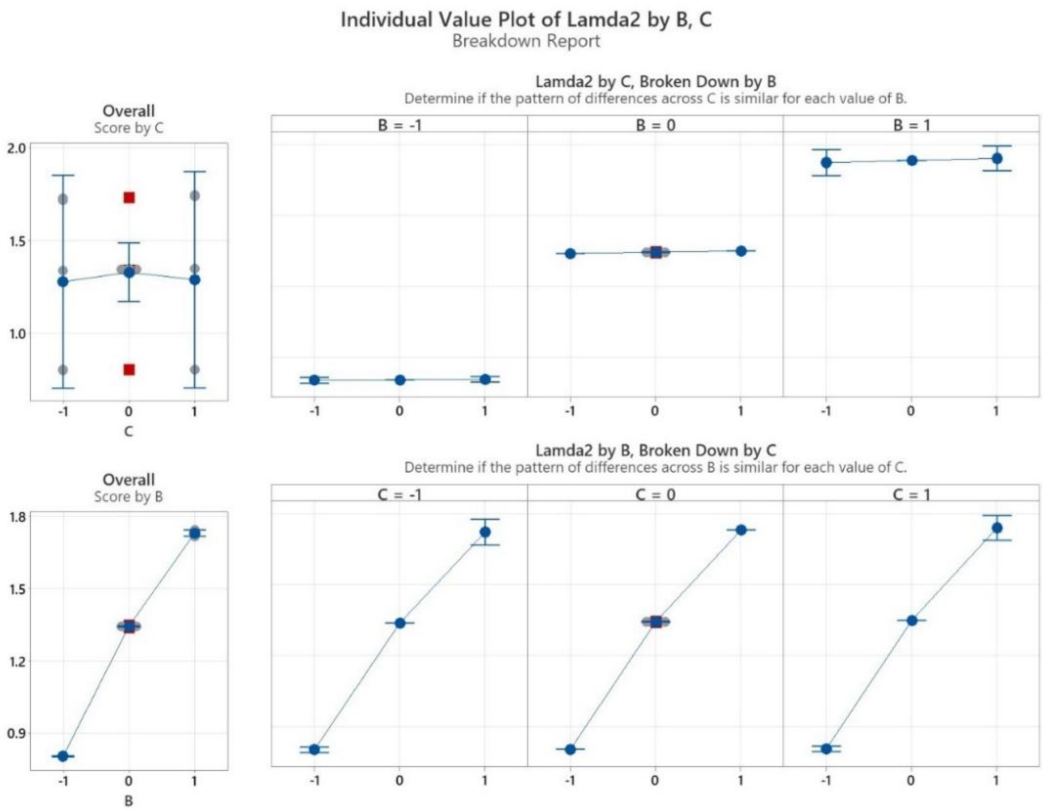

Figure 4: Sensitivity Analysis for case $\lambda_2 = 0.7$

5. Conclusions

A comprehensive computational and statistical investigation has been carried out for tetra hybrid nanofluid flow over a convectively heated moving surface with internal heat generation. The bvp4c numerical results clearly capture the dual solution behaviour and highlight the effects of Biot number, suction parameter, and heat generation on heat transfer. Statistical evaluation via RSM confirms the Biot number as the most influential factor, with suction and heat generation exerting secondary but meaningful effects. The novelty of this work lies in combining high-fidelity boundary layer solutions with a rigorous sensitivity analysis to uncover the hierarchy of parameter influence for a tetra hybrid nanofluid, a configuration scarcely investigated to date. The results demonstrate that optimal tuning of the Biot number and suction can markedly enhance heat transfer while preserving flow stability. This study provides a computational reference for multi-nanoparticle systems and offers direct engineering guidance for heat exchangers, cooling technologies, and manufacturing processes involving moving heated surfaces. Future extensions may incorporate unsteady effects, magnetic field interactions or experimental validation to bridge theory and application.

Acknowledgements

The research and financial supports are from Universiti Teknikal Malaysia Melaka (UTeM), Malaysia.

References

Abdelmalek Z., Mahanthesh B., Basir M.F.M., Imtiaz M., Mackolil J., Khan N.S., Nabwey H.A. & Tlili I. 2020. Mixed radiated magneto Casson fluid flow with Arrhenius activation energy and Newtonian heating effects: Flow and sensitivity analysis. *Alexandria Engineering Journal* **59**(5): 3991–4011.

Alsemiry R.D., Ahmed S.E., Eid M.R. & Elsaid E.M. 2025. ANN-based prediction and RSM optimization of radiative heat transfer in couple stress nanofluids with thermodiffusion effects. *Processes* **13**(4): 1055.

Choi S.U.S. & Eastman J.A. 1995. Enhancing thermal conductivity of fluids with nanoparticles. *ASME Fluids Engineering Division* **231**: 99–105.

Elsherbiny M.S., Ali M., Shahin M. & El-Kady M. 2025. Experimental study on the effect of micro concentrations of hybrid nanofluids through microchannel heat sinks. *Journal of Applied and Computational Mechanics* **11**(2): 303–326.

Khan D., Kumam P., Watthayu W. & Jarad F. 2024. Exploring the potential of heat transfer and entropy generation of generalized dusty tetra hybrid nanofluid in a microchannel. *Chinese Journal of Physics* **89**: 1009–1023.

Khashi'ie N.S., Arifin N.M. & Pop I. 2022. Magnetohydrodynamics (MHD) boundary layer flow of hybrid nanofluid over a moving plate with Joule heating. *Alexandria Engineering Journal* **61**(3): 1938–1945.

Khashi'ie N.S., Waini I., Hamzah K.B., Mukhtar M.F., Kasim A.R.M., Arifin N.M. & Pop I. 2023. Numerical solution and statistical analysis of the unsteady hybrid ferrofluid flow with heat generation subject to a rotating disk. *ZAMM–Journal of Applied Mathematics and Mechanics* **103**(6): e202200384.

Khashi'ie N.S., Mukhtar M.F., Abdollah M.F., Arifin N.M. & Pop I. 2025. Response surface-based optimization and sensitivity analysis of MHD tetra hybrid nanofluid flow over a shrinking disk. *Chinese Journal of Physics* **96**: 228–244.

Mahanthesh B. & Thriveni K. 2021. Nanoparticle aggregation effects on radiative heat transport of nanoliquid over a vertical cylinder with sensitivity analysis. *Applied Mathematics and Mechanics* **42**(3): 331–346.

Mahariq I., Khan D., Ghazwani H.A. & Shah M.A. 2024. Enhancing heat and mass transfer in MHD tetra hybrid nanofluid on solar collector plate through fractal operator analysis. *Results in Engineering* **24**: 103163.

Maruda R.W., Arkusz K., Szczotkarz N., Wojciechowski S., Niesłony P. & Królczyk G.M. 2023. Analysis of size and concentration of nanoparticles contained in cutting fluid during turning of 316L steel in minimum quantity lubrication conditions. *Journal of Manufacturing Processes* **87**: 106–122.

Maskeen M.M., Zeeshan A., Mehmood O.U. & Hassan M. 2019. Heat transfer enhancement in hydromagnetic alumina–copper/water hybrid nanofluid flow over a stretching cylinder. *Journal of Thermal Analysis and Calorimetry* **138**: 1127–1136.

Mehmood T., Ramzan M., Howari F., Kadry S. & Chu Y.M. 2021. Application of response surface methodology on the nanofluid flow over a rotating disk with autocatalytic chemical reaction and entropy generation optimization. *Scientific Reports* **11**(1): 4021.

Modi K.V., Patel P.R. & Patel S.K. 2023. Applicability of mono-nanofluid and hybrid-nanofluid as a technique to improve the performance of solar still: A critical review. *Journal of Cleaner Production* **387**: 135875.

Oladapo O.A., Ajala O.A., Akindele A.O., Aselebe L.O., Obalalu A.M., Ohaegbue A.D. & Adegbite P. 2024. Analysis of variable properties on ternary and tetra hybrid nanofluids using Blasius Rayleigh-Stokes time dependent variable: A model for solar aeronautical engineering. *International Journal of Thermofluids* **23**: 100775.

Panda S., Ontela S., Mishra S.R. & Pattnaik P.K. 2023. Response surface methodology and sensitive analysis for optimizing heat transfer rate on the 3D hybrid nanofluid flow through permeable stretching surface. *Journal of Thermal Analysis and Calorimetry* **148**(14): 7369–7382.

Reddy M.G. & Reddy K.V. 2015. Influence of Joule heating on MHD peristaltic flow of a nanofluid with compliant walls. *Procedia Engineering* **127**: 1002–1009.

Sahoo R.R. & Kumar V. 2020. Development of a new correlation to determine the viscosity of ternary hybrid nanofluid. *International Communications in Heat and Mass Transfer* **111**: 104451.

Shutaywi M., Raza J., Lund L.A., Shah Z., Vrinceanu N. & Deebani W. 2024. Optimization of heat transfer in a channel with stretching walls using a magnetized tetra-hybrid nanofluid. *Advances in Mechanical Engineering* **16**(11): 16878132241293959.

Vahedi S.M., Ghadi A.Z. & Valipour M.S. 2018. Application of response surface methodology in the optimization of magneto-hydrodynamic flow around and through a porous circular cylinder. *Journal of Mechanics* **34**(5): 695–710.

Venkatadri K., Öztop H.F., Prasad V.R., Parthiban S. & Bég A.O. 2024. RSM-based sensitivity analysis of hybrid nanofluid in an enclosure filled with non-Darcy porous medium by using LBM method. *Numerical Heat Transfer, Part A: Applications* **85**(6): 875–899.

Wahid N.S., Mustafa M.S., Arifin N.M., Pop I., Anuar N.S. & Khashi'ie N.S. 2024. Numerical and statistical analyses of three-dimensional non-axisymmetric Homann's stagnation-point flow of nanofluids over a shrinking surface. *Chinese Journal of Physics* **89**: 1555–1570.

Wahid N.S., Mustafa M.S., Arifin N.M., Khashi'ie N.S. & Pop I. 2025a. Hybrid nanofluid radiative flow across a permeable convective moving surface with heat generation: Numerical and statistical approach. *Neural Computing and Applications* **37**(5): 2911–2923.

Wahid N.S., Abu Bakar S., Mustafa M.S., Md Arifin N. & Pop I. 2025b. Magnetohydrodynamic ternary hybrid nanofluid slip flow past a permeable shrinking sheet: Boundary layer flow control and optimization using response surface methodology. *International Journal of Numerical Methods for Heat & Fluid Flow* **35**(3): 1071–1092.

Wahid N.S., Mustafa M.S., Arifin N.M., Khashi'ie N.S. & Pop I. 2025c. Hybrid nanofluid radiative flow across a permeable convective moving surface with heat generation: Numerical and statistical approach. *Neural Computing and Applications* **37**(5): 2911–2923.

Weidman P.D., Kubitschek D.G. & Davis A.M. 2006. The effect of transpiration on self-similar boundary layer flow over moving surfaces. *International Journal of Engineering Science* **44**(11-12): 730–737.

Yahaya R.I., Arifin N.M., Pop I., Ali F.M. & Isa S.S.P.M. 2024. Hybrid nanofluid flow over a shrinking rotating disk: Response surface methodology. *Computation* **12**(7): 141.

Yahaya R.I., Mustafa M.S., Md Arifin N., Md Ali F. & Mohamed Isa S.S.P.M. 2025. Heat transfer optimization for the unsteady mixed convection flow of hybrid nanofluid over a permeable EMHD riga plate with thermal radiation and convective boundary condition. *Multiscale and Multidisciplinary Modeling, Experiments and Design* **8**(3): 192.

Yan L., Dero S., Khan I., Mari I.A., Baleanu D., Nisar K.S., Sherif E.S.M. & Abdo H.S. 2020. Dual solutions and stability analysis of magnetized hybrid nanofluid with joule heating and multiple slip conditions. *Processes* **8**(3): 332.

Yaseen M., Kumar M. & Rawat S.K. 2021. Assisting and opposing flow of a MHD hybrid nanofluid flow past a permeable moving surface with heat source/sink and thermal radiation. *Partial Differential Equations in Applied Mathematics* **4**: 100168.

Zainal N.A., Nazar R., Naganthran K. & Pop I. 2021. MHD flow and heat transfer of hybrid nanofluid over a permeable moving surface in the presence of thermal radiation. *International Journal of Numerical Methods for Heat & Fluid Flow* **31**(3): 858–879.

Zhang Z., Wang X. & Yan Y. 2021. A review of the state-of-the-art in electronic cooling. *e-Prime – Advances in Electrical Engineering, Electronics and Energy* **1**: 100009.

Fakulti Teknologi dan Kejuruteraan Mekanikal
Universiti Teknikal Malaysia Melaka
Hang Tuah Jaya, 76100 Durian Tunggal
Melaka, MALAYSIA
E-mail: najiyah@utem.edu.my, mohdfadzli@utem.edu.my*

Fakulti Pengurusan Teknologi dan Teknousahawanan
Universiti Teknikal Malaysia Melaka
Hang Tuah Jaya, 76100 Durian Tunggal
Melaka, MALAYSIA
E-mail: fariduddin@utem.edu.my

Department of Mathematics and Statistics
Faculty of Science
Universiti Putra Malaysia
43400 UPM Serdang
Selangor, MALAYSIA
E-mail: norihana@upm.edu.my

Department of Mathematics
Babeş-Bolyai University
R-400084 Cluj-Napoca
ROMANIA
E-mail: popm.ioan@yahoo.co.uk

Received: 16 August 2025
Accepted: 25 October 2025

*Corresponding author